RINGOSTAR: An Evolutionary AWG-Based WDM Upgrade of Optical Ring Networks

Martin Herzog, Martin Maier, *Member, IEEE*, and Adam Wolisz, *Senior Member, IEEE*

***Abstract*—The paper describes the study of the multichannel upgrade of IEEE Standard 802.17 Resilient Packet Ring (RPR) in particular and optical single-channel ring networks in general by making use of wavelength-division multiplexing (WDM). The paper describes and discusses a novel evolutionary multichannel upgrade approach that uses WDM on a central passive arrayed-waveguide grating (AWG)-based single-hop star network rather than on the ring. The AWG-based star subnetwork allows for a dramatically larger spatial reuse of WDM wavelength channels than conventional upgrades of optical single-channel ring networks that use WDM on the ring where *all* nodes need to be WDM upgraded. In the resultant hybrid optical ring-star network, termed RINGOSTAR, only a *subset* of the nodes are required to be WDM upgraded with a single additional tunable transceiver in order to improve the performance dramatically. The novel concept of *proxy stripping* is also introduced, which is used to route ring traffic on single-hop short cuts across the star subnetwork rather than the peripheral ring, resulting in a dramatically increased spatial reuse factor on the ring. By means of analysis, the performance of RINGOSTAR is investigated in terms of mean hop distance, spatial reuse, and capacity. The findings show that RINGOSTAR significantly outperforms unidirectional, bidirectional, and meshed WDM rings. Finally, the tradeoffs of RINGOSTAR are addressed.**

***Index Terms*—Arrayed-waveguide grating (AWG), buffer insertion rings, destination stripping, empty slot access, medium access control (MAC), meshed rings, metropolitan area networks (MANs), optical–electrical–optical (O/E/O), OOO, Resilient Packet Ring (RPR), source stripping, spatial reuse, WDM.**

I. Introduction

THE new Resilient Packet Ring (RPR) IEEE Standard 802.17 aims at improving the channel utilization, throughput efficiency, service differentiation, and resilience of optical single-channel packet-switched ring metropolitan area networks (MANs). Prestandard products have already been deployed in operational metro networks. This paper addresses the multichannel extension of RPR in particular and optical single-channel ring networks in general by using wavelength-division multiplexing (WDM). To date, a plethora of WDM MANs have been proposed and investigated. Typically, these WDM MANs have either a ring or star topology [1]. Both topologies have their own merits and drawbacks. Rings are primarily used for their fault tolerance against any single node or fiber failure. On the downside, traffic generally has to traverse multiple intermediate ring nodes—either optically bypassing them or being stored and forwarded by them—on its way to the destination, as opposed to single-hop star networks. Thus, traffic consumes more bandwidth resources in ring networks than in single-hop star networks. As a result, rings are inherently less bandwidth efficient than star networks, especially in the face of today's situation where service providers often lease dedicated point-to-point high-speed lines to customers for interconnecting their geographically distributed sites, which naturally calls for a star rather than a ring configuration. Furthermore, single-hop star networks inherently provide transparency to bit rate, modulation format, and protocol. Consequently, they are able to easily support not only legacy but also future protocols. On the other hand, star topologies also suffer from a number of shortcomings. In general, star networks require a larger amount of fiber quantities than their ring counterparts, and the central hub forms a single point of failure.

In this paper, a novel hybrid ring-star architecture termed RINGOSTAR is proposed and examined. RINGOSTAR not only aims at combining the aforementioned strengths of both ring and star configurations while avoiding their drawbacks but also follows an entirely new direction to WDM upgrade optical single-channel rings. Instead of deploying WDM on the ring, RINGOSTAR uses WDM on the central arrayed-waveguide grating (AWG)-based single-hop star network, thereby exploiting the large spatial wavelength reuse capability of the wavelength-routing AWG. Generally, in RINGOSTAR, only a subset of ring nodes is directly connected to the star network, resulting in less fiber requirements and node interfaces.

The remainder of the paper is organized as follows. Section II provides an overview of performance enhancing mechanisms for optical single-channel ring networks and describes their use in RPR. In Section III, we briefly highlight the previous work on WDM upgrades of optical single-channel rings. The AWG-based single-hop star WDM network is described in greater detail in Section IV. Section V describes the RINGOSTAR network and node architecture and the medium access control (MAC) protocol. In Section VI, the performance of RINGOSTAR is examined by means of analysis, and it is compared to that of unidirectional, bidirectional, and meshed WDM rings. Section VII concludes the paper.

II. Optical Single-Channel Ring Networks

Optical single-channel ring networks belong to the first generation of *opaque* optical networks where optical–elec-

Manuscript received September 10, 2004; revised December 7, 2004. This work was supported in part by the European Commission within the Network of Excellence e-Photon/ONe and the German research funding agency Deutsche Forschungsgemeinschaft (DFG) under the graduate program 'Graduiertenkolleg 621 (MAGSI/Berlin).

M. Herzog and A. Wolisz are with the Telecommunication Networks Group, Technical University Berlin, 10587 Berlin, Germany (e-mail: herzog@tkn.tu-berlin.de; awo@ieee.org).

M. Maier is with the Centre Tecnològic de Telecomunicacions de Catalunya (CTTC), 08034 Barcelona, Spain (e-mail: martin.maier@cttc.es; website: http://www.cttc.es).

Digital Object Identifier 10.1109/JLT.2005.844501

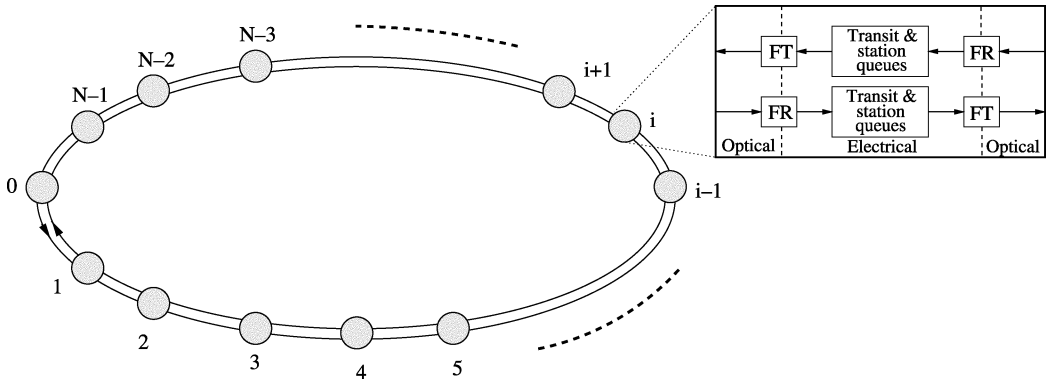

Fig. 1. Generic RPR network and node architecture connecting N nodes.

trical–optical (O/E/O) conversion takes place at each node [2]. Among others, the Cambridge ring is a *unidirectional* ring network [3]. Channel access is based on the *empty slot* principle. The Cambridge ring deploys *source stripping* where the source node takes the transmitted packet from the ring. The buffer insertion ring is a *unidirectional* ring network [4] where each node temporarily stores the incoming ring traffic in the electrical insertion buffer in order to allow the local node to transmit a packet onto the ring.

In both unidirectional ring networks, the maximum hop distance equals $h_{\max} = N - 1$, where N denotes the number of nodes in the network. As opposed to the Cambridge ring, however, packets are removed from the buffer insertion ring by the receiving node (rather than the transmitting node). This so-called *destination stripping* enables downstream nodes to *spatially reuse* bandwidth and decreases the mean hop distance of the ring network. For uniform traffic, i.e., each node generates the same amount of traffic, and a given packet is destined to any of the $(N-1)$ nodes with equal probability $1/(N-1)$, the mean hop distance of destination stripping rings is given by

$$\overline{h} = \frac{1}{N-1}\sum_{j=1}^{h_{\max}} j = \frac{1}{N-1}\sum_{j=1}^{N-1} j = \frac{N}{2}. \tag{1}$$

Due to the decreased mean hop distance and spatial reuse, the average throughput of the network is improved by a factor of up to two.

Unlike the aforementioned ring networks, MetaRing is a dual-fiber *bidirectional* full-duplex ring operating either in the buffer insertion mode for variable-size packets or slotted mode for fixed-size packets/cells where the slot size equals the transmission time of a fixed-size packet/cell [5]. Nodes deploy destination stripping. Furthermore, packets are transmitted via the *shortest path* by choosing the appropriate ring. With destination stripping and shortest path routing, the maximum hop distance is equal to $h_{\max} = \lceil (N-1)/2 \rceil$. For uniform traffic, the mean hop distance of bidirectional destination stripping rings with shortest path routing is given by

$$\overline{h} = \frac{2}{N-1}\sum_{j=1}^{\lfloor \frac{N-1}{2} \rfloor} j + \frac{(N-1) \bmod 2}{N-1}\left\lceil \frac{N-1}{2} \right\rceil \tag{2}$$

$$= \begin{cases} \frac{N+1}{4} & \text{if } N \text{ odd} \\ \frac{N^2}{4(N-1)} & \text{if } N \text{ even} \end{cases} \tag{3}$$

where $\lceil \cdot \rceil$ and $\lfloor \cdot \rfloor$ denote the ceiling function and floor function, respectively. Due to the decreased mean hop distance, the spatial reuse factor equals four, i.e., for uniform traffic, the average throughput is improved by a factor of up to four.

Various aspects of the previously mentioned ring networks can be found in the new standard RPR for high-performance packet-switched optical single-channel MANs [6], [7]. As shown in Fig. 1, RPR is a bidirectional dual-fiber ring network with O/E/O conversion at each of the N nodes. Every node is equipped with two fixed-tuned transmitters (FTs) and two fixed-tuned receivers (FRs), one for each fiber ring. Broadcasting is achieved by means of source stripping. Destination stripping in conjunction with shortest path routing improves the spatial reuse of bandwidth significantly. Note, however, that the path selection in IEEE Standard 802.17 is not necessarily shortest path routing. Higher layers (such as Internet protocol (IP)) may explicitly specify the "best" direction/ring to each destination, including shortest path [8]. Each node has separate transit and station queues for either ring, as depicted in Fig. 1. Specifically, for each ring, a node has one or two transit queues: one transmission queue termed *stage queue*, one reception queue, and one add_MAC queue, which stores control packets generated by the local node.

RPR nodes operate in one of two modes: 1) single-queue mode or 2) dual-queue mode. In single-queue mode, the transit path consists of a single first-in first-out (FIFO) queue termed the *primary transit queue* (PTQ). If the PTQ is not full, highest priority is given to add_MAC traffic. At the absence of local control traffic, priority is given to in-transit ring traffic over station traffic. In dual-queue mode, the transit path comprises two queues, one for guaranteed Class A traffic (PTQ) and one secondary transit queue (STQ) for Class B (committed rate) and Class C (best effort) traffic. In dual-queue mode, if both PTQ and STQ are not full, highest priority is given to add_MAC traffic (similar to single-queue mode). If there is no local control traffic, PTQ traffic is always served first. If the PTQ is empty, the local transmission queue (stage queue) is served until STQ reaches a certain queue threshold. If STQ reaches that threshold, the STQ in-transit ring traffic is given priority over station traffic such that in-transit packets are not lost due to buffer overflow. Thus, the transit path is lossless, and a packet put on the ring

is not dropped at downstream nodes. Furthermore, RPR defines fairness control algorithms that specify how a congested downstream node can throttle the transmission rate of upstream nodes by sending fairness control packets upstream.

This paper does not focus on the performance improvement of the single-channel RPR architecture and protocols. Instead, we examine the *multichannel* extension of RPR in particular and optical single-channel ring networks in general. More precisely, we investigate how WDM can be used to efficiently upgrade RPR and optical single-channel ring networks.

III. Ring WDM Upgrades: Previous Work

For a comprehensive survey on and an in-depth discussion of WDM upgraded ring networks and access protocols, including fairness control and quality of service (QoS) support, the interested reader is referred to [9]. In the following, we briefly review the most important improvements of optical ring networks to increase the capacity of ring WDM networks, where the capacity denotes the maximum achievable throughput of the network.

A. All-Optical Node Structures

Instead of O/E/O converting all signals at each node, *all-optical* node structures have been proposed which leave the data packets in the optical domain while processing the packet header information in the electrical domain to decide whether to drop or forward the data packet [10], [11]. In doing so, only packets destined for the local node have to be O/E converted while in-transit traffic remains in the optical domain. Note, however, that these all-optical (OOO) nodes do not necessarily provide logical optical bypasses, as discussed in the subsequent section.

B. Optical Bypassing and Traffic Grooming

With *optical bypassing*, each node has to inspect/process only a subset of the wavelengths while the remaining wavelengths pass through the node untouched, resulting in a decreased computational burden and reduced number of electronic port cards at bypassed nodes. The required number of electronic port cards and wavelengths can be further reduced by means of *grooming* [12]–[14]. More importantly, optical bypassing enables the design of *logical* topologies that are embedded on the physical ring network [15], [16]. By optically bypassing nodes, the mean hop distance of logical topologies can be decreased.

Note that in logical topologies, the *logical* maximum and mean hop distance between nodes is decreased, but the *physical* path remains unchanged. Hence, traffic consumes the same amount of bandwidth resources no matter whether optical bypassing is provided or not. As a consequence, in WDM ring networks—either with or without optical bypassing—the spatial reuse factor is no larger than in their single-channel counterparts.

C. Meshed Rings

The spatial reuse factor in bidirectional WDM rings can be increased by providing *alternate* physical paths in addition to the fiber rings, resulting in so-called *meshed rings* [17], [18]. In addition to the ring nodes, wavelength routers are equally distributed on the bidirectional ring, which are interconnected by counterdirectional pairs of fiber called *chords*. In doing so, physical short cuts are created that allow the sending of data packets while skipping all intermediate ring nodes between two connected wavelength routers, resulting in an increased spatial reuse on the ring. It was shown in [17] and [18] that, for uniform traffic, a meshed ring using $K = 6$ wavelength routers and $W = 5$ wavelengths increases the network capacity by 720% compared with unidirectional source stripping rings, which translates into a spatial reuse factor of 7.2. Note that chords are limited in further decreasing the mean hop distance of meshed rings. To see this, recall that each chord provides a short cut between two wavelength routers. Each chord interconnects a different pair of wavelength routers. In general, a data packet has to traverse multiple chords in order to reach its destination. This is due to the fact, that each chord acts as a stand-alone short cut of limited range in that each chord provides a short cut to a single wavelength router, which in general is not the one closest to the final destination node. As a consequence, data packets generally travel along multiple hops on their way from a given source node to a given destination node. As we will see shortly, our approach avoids multihopping by interconnecting all chords through a central hub in a single-hop subnetwork such that a given wavelength router is able to use its locally attached chord to get access to the central hub and thereby to all other chords attached to the hub. Thus, a given source node is able to send packets to the wavelength router that is closest to the corresponding destination node, resulting in a decreased mean hop distance and an increased capacity. (Note that multihopping in meshed rings could also be prevented by interconnecting all wavelength routers in a full mesh. As opposed to our approach, however, this method requires a prohibitively large number of fibers (chords) for interconnecting multiple wavelength routers.)

In the following, we propose and investigate an entirely different approach to WDM upgrade RPR and optical single-channel rings. In our approach, we use a single wavelength router functioning as a central hub as opposed to meshed rings, which use multiple wavelength routers placed on the bidirectional ring. Furthermore, we do not apply WDM on the ring as done in the aforementioned WDM upgrades of optical single-channel ring networks. Instead, WDM is used only on the central-wavelength-router-based single-hop star network while leaving the peripheral fiber rings unchanged.

Next, let us first take a closer look at the central-wavelength-router-based single-hop star WDM network and the resultant hybrid ring-star network architecture. After describing them in greater detail in the following two sections, we return to meshed rings in Section V-D, when contrasting our approach to the previously mentioned WDM upgrades of optical single-channel ring networks.

IV. AWG-Based Star WDM Network

The wavelength router we use in this paper is a frequency-cyclic $D \times D$ AWG with D input ports and D output ports, where $D \geq 1$. Without loss of generality, we consider a 2×2 AWG to explain the properties of an AWG. Fig. 2 illustrates a scenario where six wavelengths are launched into both AWG input ports. Let us first consider only the upper input port. The AWG routes every second wavelength to the same output port.

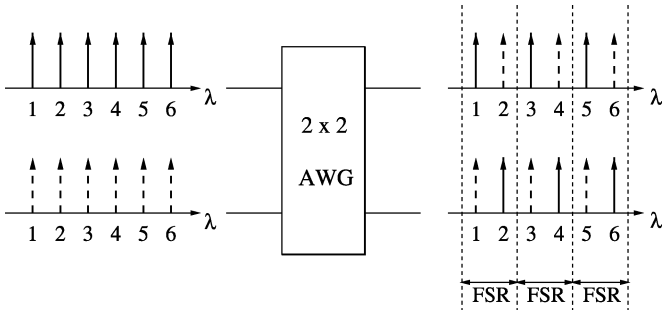

Fig. 2. Periodic wavelength routing and spatial wavelength reuse of a 2 × 2 AWG.

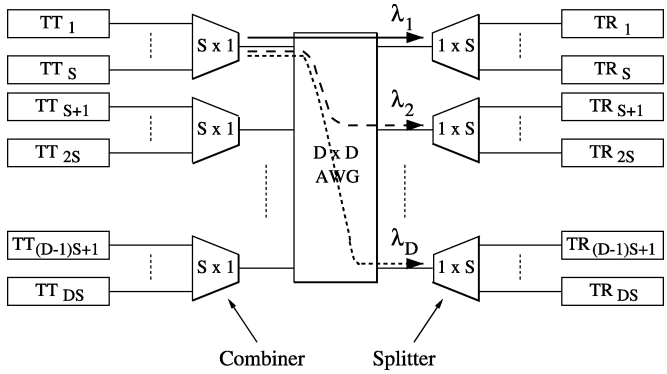

Fig. 3. Wavelength-routing $D \times D$ AWG-based star WDM network with $N_{\mathrm{AWG}} = D \cdot S$ nodes.

This period of the wavelength response is called free spectral range (FSR). In our example, there are three FSRs, each containing two wavelengths. Generally, the FSR of a $D \times D$ AWG consists of D contiguous wavelengths, i.e., the physical degree of an AWG is identical to the number of wavelengths per FSR. As shown in Fig. 2, this holds also for the lower AWG input port. Note that the AWG routes wavelengths such that no collisions occur at the AWG output ports, i.e., each wavelength can be applied at all AWG input ports simultaneously. In other words, *with a $D \times D$ AWG, each wavelength can be spatially reused D times*. In addition, note that each FSR provides one wavelength channel for communication between a given pair of AWG input and output ports. Hence, using R FSRs allows for R simultaneous transmissions between each AWG input–output port pair, and the total number of wavelength channels available at each AWG port is given by $\Lambda = R \cdot D$, where $R \geq 1$.

The AWG can be used to design a wavelength-routing single-hop star WDM network, as shown in Fig. 3. At each input port of the $D \times D$ AWG, a wavelength-insensitive $S \times 1$ combiner collects data from S attached tunable transmitters (TTs), where $S \geq 1$. By setting $S \geq 1$, multiple transmissions can take place simultaneously at each AWG port, each at a different wavelength resulting in WDM. Similarly, at each AWG output port, signals are equally distributed to S attached tunable receivers (TRs) by a wavelength-insensitive $1 \times S$ splitter. These wavelength-insensitive splitters also enable optical multicasting since each splitter locally broadcasts packets to all respective S nodes. Let each transmitter and the opposite located receiver belong to a different node. In doing so, the number of network nodes equals $N_{\mathrm{AWG}} = D \cdot S$. To maintain unrestrained connections between any pair of AWG input port and AWG output port, we assume that both the TT and TR of each node are tunable over the aforementioned $\Lambda = R \cdot D$ wavelength channels.

Given that both the transmitter and receiver of each node are tunable, it is reasonable to arbitrate the wavelength channel access by means of a reservation protocol with pretransmission coordination. For an in-depth discussion and performance evaluation of a distributed attempt-and-defer type of reservation protocol for an AWG-based single-hop star WDM network, the interested reader is referred to [19] and [20].

V. RINGOSTAR

In this section, we describe how the AWG-based single-hop star network of Section IV is used to provide an efficient WDM upgrade of RPR in particular and optical single-channel rings in general. We also introduce the applied MAC protocol. We call the resultant hybrid optical ring-star network RINGOSTAR.

A. Related Work

The combination of star and ring configurations to form hybrid network topologies has already been addressed to some extent previously.

Bellcore's Star-Track switch is formed from two internal networks, an optical passive star coupler (PSC)-based broadcast-and-select single-hop star WDM network and an electronic unidirectional token-based control ring [21], [22]. To access the star network, each node has one FT and one TR. The control token ring is used for making reservations. After one ring round-trip propagation delay, data packets are sent across the star. Star-Track does not allow for immediate ring access due to the token based protocol. Moreover, the PSC as a broadcast device does not support spatial wavelength reuse, as opposed to the wavelength-routing AWG.

A hybrid star-ring network based on multiple central wavelength routers in parallel was proposed in [23]. All ring nodes are connected to the central wavelength routers by either one or two pairs of fiber (so-called *spokes*). In addition, ring nodes are interconnected by a small number of fibers around the circumference carrying protection-switched traffic to standby spokes as well as residual working wavelength channels. The use of additional fibers in a ring around the periphery of the multiple-star network is one of the key features that allows total fiber quantities to be minimized. It was shown that for a single path failure and uniform traffic, fiber requirements are less than for a WDM add–drop multiplexer (ADM) ring, while providing greater resilience to multiple path failures. The work focused primarily on path and wavelength router protection strategies and did not specify any MAC protocol. Furthermore, the architecture does not deploy splitters for enabling optical multicasting.

A multilevel star-ring architecture consisting of a star network on the upper level and multiple concatenated ring subnets on the lower level was studied in [24]. The upper level star network ensures high network capacity, and its weakness in reliability is overcome by the concatenated ring subnets with self-healing capabilities. The work concentrates on the physical transmission limitations rather than protocols. Again, a MAC

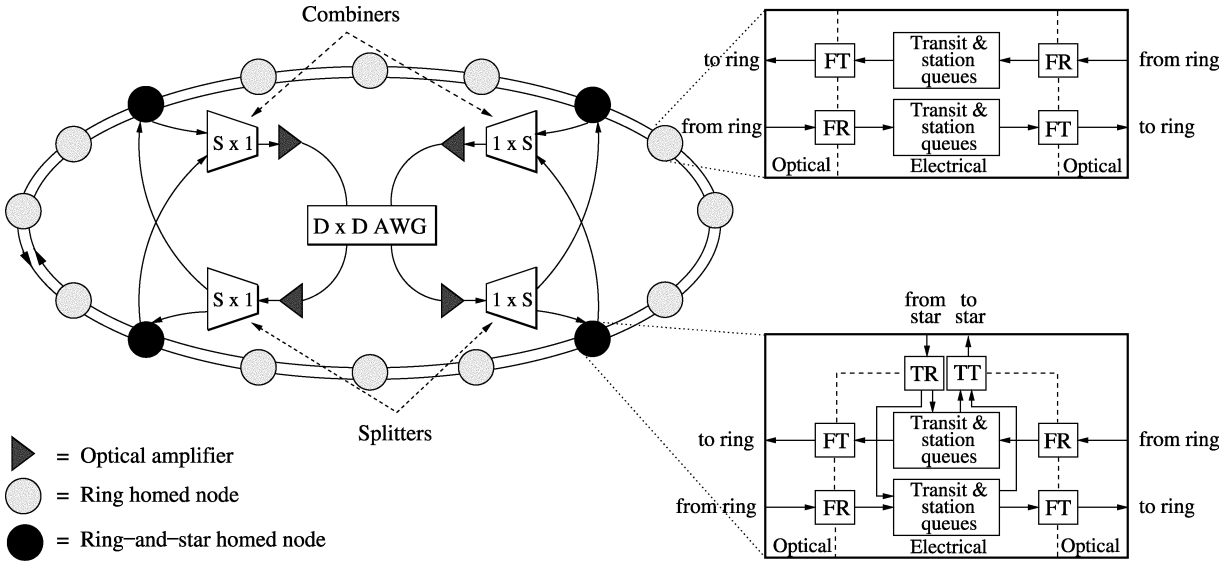

Fig. 4. RINGOSTAR network and node architecture with $N = 16$ and $D = S = 2$.

protocol for such a modified star-ring architecture was not provided and investigated.

RINGOSTAR differs from the previously mentioned ring-star architectures in a number of ways. As we will see shortly, RINGOSTAR deploys a single wavelength router (AWG) with attached splitters to enable optical multicasting. In general, only a subset of the ring nodes are directly connected to the star network. The MAC protocol allows for immediate medium access on the bidirectional ring. The integrated ring-star network forms a single-level architecture. Both the RINGOSTAR architecture and MAC protocol are explained next.

B. Architecture

1) Network Architecture: RINGOSTAR interconnects N nodes, which are subdivided into two groups of $N_{\mathrm{rs}} = D \cdot S$ ring-and-star homed nodes and $N_r = N - D \cdot S$ ring homed nodes, where $N = N_r + N_{\mathrm{rs}}$, $D \geq 1$, $S \geq 1$, and $N \geq 1$. All N nodes are attached to a bidirectional dual-fiber ring by means of two fixed-tuned transceivers, one for each single-channel fiber. The N_{rs} ring-and-star homed nodes are equally distributed among the N_r ring homed nodes on the ring, as shown in Fig. 4 for $N = 16$ and $N_{\mathrm{rs}} = 4$ (and $N_r = N - N_{\mathrm{rs}} = 12$). Unlike the ring homed nodes, the ring-and-star homed nodes are also attached to the central AWG-based star network by using an additional tunable transceiver and fiber pair. More precisely, the TT of a given ring-and-star homed node is connected to a combiner input port, and its TR is located at the opposite splitter output port. Thus, the number of ring-and-star homed nodes is given by $N_{\mathrm{rs}} = D \cdot S \leq N$. Generally, for a given N_{rs} different combinations of D and S are possible, e.g., $D = S = 2$ for $N_{\mathrm{rs}} = 4$, as shown in Fig. 4. If necessary, an optical amplifier, e.g., Erbium-doped fiber amplifier (EDFA), is placed between each combiner and AWG input port and each AWG output port and splitter to compensate for fiber, splitting, and insertion losses in the star network. In summary, the structure of each ring homed and ring-and-star homed node is $\mathrm{FT}^2 - \mathrm{FR}^2$ and $\mathrm{FT}^2 - \mathrm{TT} - \mathrm{FR}^2 - \mathrm{TR}$, respectively, and is discussed in greater detail in the subsequent section.

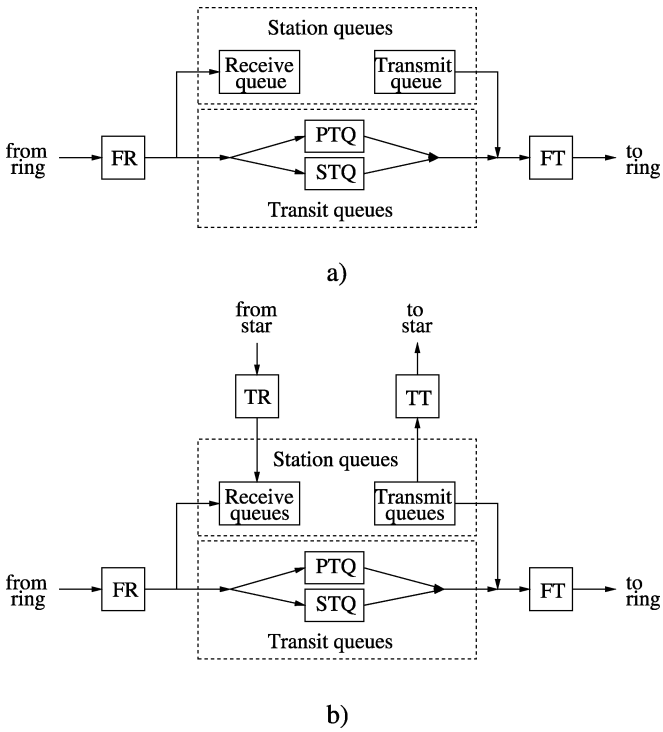

Fig. 5. RINGOSTAR node architecture for either fiber ring: (a) ring homed node and (b) ring-and-star homed node.

2) Node Architecture: Similar to RPR, each node performs O/E/O conversion and has separate electrical transit and station queues for either fiber ring. In the case of ring-and-star homed nodes, the station queues are also connected to the star transceiver, as depicted in Fig. 4. Fig. 5 shows the buffer structure in greater detail for both ring and ring-and-star homed nodes. (We show only the buffers for one fiber ring. The same buffer structure is replicated at each node for the other counterdirectional fiber.) Fig. 5(a) depicts the architecture of ring homed nodes. Similar to RPR, each ring homed node is equipped with two transit (PTQ for high-priority traffic and STQ for low-priority traffic) and two station (receive and transmit) queues. Sim-

ilarly, ring-and-star homed nodes have the same transit and station queues, as well as two additional station (one transmit and one receive) queues to store data packets going to and coming from the star, as illustrated in Fig. 5(b).

C. MAC Protocol

The MAC protocol in RINGOSTAR makes use of the aforementioned features of RPR. In the following, we first explain the underlying principles and then describe the operation of the MAC protocol.

1) Underlying Principles: In RINGOSTAR, all N nodes use the RPR dual-queue scheduling algorithm to arbitrate service among transit and station queues on the ring, as outlined in Section II. Accordingly, intermediate ring nodes store packets arriving on the ring in one of the two transit queues according to the packets' priority. Control packets have high priority and are thus stored in the PTQ buffer. There are three basic principles used in the RINGOSTAR access protocol.

1) Source stripping is used for broadcasting control packets (and data packets, if required).
2) Destination stripping is used for unicast data packets.
3) *Proxy stripping* is a novel concept in RINGOSTAR and is used only by ring-and-star homed nodes. With proxy stripping, ring-and-star homed nodes that are neither source nor destination pull incoming data packets from the ring and send them across single-hop short-cuts on the AWG based star network to other ring-and-star homed nodes. (Practically, this can be done by monitoring each packet's source and destination MAC addresses and making a table lookup at proxy stripping nodes with table entries indicating whether a given data packet has to be proxy stripped or not.) The receiving ring-and-star homed nodes are either the destination of the data packets or closest to the corresponding destination ring homed node. In the latter case, the receiving ring-and-star homed node forwards the data packets on the shortest path by choosing the appropriate fiber ring. The destination ring homed node finally takes the data packets from the ring (destination stripping).

2) Operation: The MAC protocol aims at maximizing the capacity of the RINGOSTAR network. In the multihop RINGOSTAR network, only a portion of the network capacity is used for newly generated traffic. A certain amount of network capacity is taken up by forwarded traffic as packets hop from one node to another in order to get to their destinations. The network capacity C is inversely proportional to the average number of hops (mean hop distance) that a packet takes to get to its destination [25]

$$C \propto \frac{1}{E[\text{hops}]}. \tag{4}$$

Clearly, to maximize C, the mean hop distance has to be minimized. To this end, all nodes have to send data packets on the shortest path in terms of hop counts. In doing so, the forwarding burden of nodes is alleviated and a larger amount of network capacity is available for nodes to send locally generated traffic. Let one hop denote the distance between two adjacent nodes. Adjacent nodes can be either two neighboring nodes on the ring or two nodes interconnected via the single-hop star subnetwork (this holds only for ring-and-star homed nodes). The mean hop distance denotes the average value of the minimum numbers of hops a data packet has to make on its shortest path from any source node to all remaining $(N-1)$ destination nodes.

Next, we specify the shortest path routing for both ring and ring-and-star homed nodes. We define the following variables for a given pair of source node s and destination node d, where $s, d \in \{0, 1, 2, \ldots, N-1\}$:

h_{s_rs} hop distance between source node s and its closest ring-and-star homed node;

h_{d_rs} hop distance between destination node d and its closest ring-and-star homed node;

$h^{\text{ring}}_{\text{min}_{s\_d}}$ minimum hop distance between source node s and destination node d on the ring, i.e., without proxy stripping;

$h^{\text{star}}_{\text{min}_{s\_d}}$ minimum hop distance between source node s and destination node d via short cuts of star subnetwork, i.e., with proxy stripping, and note that $h^{\text{star}}_{\text{min}_{s\_d}} = h_{s\_\text{rs}} + 1 + h_{d\_\text{rs}}$.

a) Ring homed nodes: Generally speaking, if the hop distance between a given source ring homed node s and destination node d is "small enough," the ring homed node sends the data packet(s) on the ring without undergoing proxy stripping. More precisely, if $h^{\text{ring}}_{\text{min}_{s\_d}} \leq h^{\text{star}}_{\text{min}_{s\_d}}$, then source node s sends the data packet(s) to destination node d along the ring on the shortest path by choosing the appropriate fiber ring. Destination node d takes the transmitted data packet(s) from the ring (destination stripping). Note that in this case, there is no proxy stripping, i.e., intermediate ring-and-star homed nodes store and forward the data packet(s) on the ring rather than sending them across the star subnetwork. Proxy stripping takes place only if $h^{\text{ring}}_{\text{min}_{s\_d}} > h^{\text{star}}_{\text{min}_{s\_d}}$, i.e., if the short cuts form a shorter path between nodes s and d than either peripheral fiber ring. Specifically, source node s sends the data packet(s) to its closest ring-and-star homed node. Note that the chosen direction does not necessarily have to be the same as that used in shortest path routing on the ring. Recall from Section II that RPR is not restricted to shortest path routing but allows for different path selection and can thus be used to transport the packets from a ring homed node to the nearest ring-and-star homed node. The corresponding ring-and-star homed node performs proxy stripping, as described in greater detail in the following.

b) Ring-and-star homed nodes: With proxy stripping, a ring-and-star homed node takes the corresponding data packet(s) from the ring and places the data packet(s) in its star transmit queue. A given proxy-stripping ring-and-star homed node pulls only data packets from the ring whose source and destination addresses satisfy the condition $h^{\text{ring}}_{\text{min}_{s\_d}} > h^{\text{star}}_{\text{min}_{s\_d}}$. Packets in the star transmit queue are sent by using a reservation protocol with pretransmission coordination. Prior to transmitting a data packet, the corresponding ring-and-star homed node broadcasts a control packet on one of the fiber rings by means of source stripping. The control packet consists of the following three fields:

1) the source address of the proxy-stripping ring-and-star homed node;

2) the destination address of the ring-and-star homed node that is closest to destination node d;
3) the length of the corresponding data packet.

Each ring-and-star homed node receives the broadcast control packet and is thus able to acquire and maintain global knowledge of all $N_{\rm rs}$ ring-and-star homed nodes' reservation requests. Note that the control packets are sent by using RPR's high-priority traffic class service. Hence, the pretransmission coordination of the star subnetwork builds on RPR and requires neither additional hardware nor software. It was shown in [26] that the latency of high-priority (control) traffic is constant and equal to the round-trip propagation delay of the ring, even under overload conditions. As a result, all ring-and-star homed nodes receive control packets after a deterministic period of time and are able to process control packets and acquire and maintain global knowledge in a synchronized manner. Based on this global knowledge, all $N_{\rm rs}$ nodes schedule the transmission and reception of the corresponding data packets on the single-hop star subnetwork in a distributed fashion. For now, we assume a deterministic first-come-first-served and first-fit (FCFS-FF) scheduling algorithm similar to that used in [19]. Note that the chosen scheduling alogrithm is relatively simple. Its low time complexity helps avoid scalability problems in very high speed networks where each node has to process broadcast control packets [2].

We note that the previously mentioned reservation with pretransmission coordination suffers from an inefficient use of ring bandwidth and nodal processing resources since each control packet travels along the entire ring. Consequently, each control packet traverses all nodes and is processed at both ring and ring-and-star homed nodes, even though only ring-and-star homed nodes need the control information, resulting in wasted ring bandwidth and nodal processing resources. To mitigate these inefficiencies, control packets may be sent across the star subnetwork instead of the ring subnetwork. To this end, each ring-and-star homed node may be equipped with an additional (off-the-shelf) broad-band light source, e.g., light-emitting diode (LED), to send control packets to all ring-and-star homed nodes. More precisely, the broad-band optical signal is spectrally sliced by the wavelength-routing AWG such that part of the signal is routed to each AWG output port, and thus every ring-and-star homed node is able to receive the control information, while the remaining ring homed nodes are relieved from processing any pretransmission control traffic. Control channel access is arbitrated by means of Reservation ALOHA (R-ALOHA). For a technically detailed description of this signaling approach, the interested reader is referred to [20].

Alternatively, the overhead caused by the round-trip of the control packet on the ring can be reduced by deploying a (wavelength-insensitive) passive star coupler (PSC) in parallel with the AWG and broadcasting the control packet via the star subnetwork. By equipping each ring-and-star homed node with an additional fixed-tuned transceiver (instead of the broad-band light source) pretransmission control packets may be sent to all ring-and-star homed nodes on the wavelength-insensitive PSC. Again, control channel access is arbitrated by means of Reservation ALOHA (R-ALOHA). For more detailed informations and additional investigations of various failure scenarios of this star subnetwork the interested reader is referred to [31].

After transmitting a given data packet across the star, the corresponding ring-and-star homed receiving node puts the data packet into its star receive queue. If necessary, the ring-and-star homed node forwards the data packet on the ring toward the destination node d on the shortest path by using the appropriate fiber ring. Destination node d finally takes the data packet from the ring (destination stripping).

Beside forwarding and proxy stripping data packets, ring-and-star homed nodes also generate traffic. Note that in this case, we have $h_{s\_{\rm rs}} = 0$. Again, if $h^{\rm ring}_{{\rm min}_{s\_d}} \leq h^{\rm star}_{{\rm min}_{s\_d}}$, then the ring-and-star homed source node s transmits the data packet on that fiber ring, which provides the shortest path to destination node d. Otherwise, if $h^{\rm ring}_{{\rm min}_{s\_d}} > h^{\rm star}_{{\rm min}_{s\_d}}$, then the ring-and-star homed source node s sends the data packet across the star subnetwork to the corresponding ring-and-star homed node, which can be the destination itself, or if it is not the destination, it forwards the data packet onwards to node d via the shortest path ring. Similarly to proxy stripping, transmission and reception of the data packet on the star subnetwork is done by means of pretransmission coordination, as explained previously.

D. Discussion

RINGOSTAR is an *evolutionary* WDM upgrade of RPR and optical single-channel rings in that it builds on the single-channel node structure and protocols of RPR. In doing so, RINGOSTAR is able to benefit from RPR's access control, fairness control, and service differentiation, as described in Section II. In RINGOSTAR, only a subset of the ring nodes $N_{\rm rs} \leq N$ need to be upgraded in general, as opposed to previous ring WDM upgrades which affect all nodes. Thus, in RINGOSTAR, nodes can be WDM upgraded and connected to the star network via dark fibers one at a time in a *pay-as-you-grow* manner. Note that recently most conventional carriers, a growing number of public utility companies, and new network operators make use of their right-of-ways especially in metropolitan areas to build and offer so-called *dark-fiber networks* [28]. These dark-fiber providers have installed a fiber infrastructure that exceeds their current needs. The unlit (dark) fibers provide a cost-effective way to build very high capacity networks or upgrade the capacity of existing (ring) networks. Buying one's own dark fibers is a promising solution to reduce network costs as opposed to leasing bandwidth, which is an ongoing expense. Furthermore, the network evolution (instead of revolution) enables operators to provide cautious upgrades of existing networks and to realize their survival strategy in a highly competitive enviroment [29]. Moreover, O/E/O conversion at each node not only allows for 3R (reamplification, reshaping, and retiming) signal regeneration but also for packet processing such as aggregation of ring data packets for transmission across the star, which is done best in the electrical domain. Note that fast TTs with a tuning time of a few nanoseconds and (fixed-tuned) burst-mode packet receivers have been shown to be feasible [32]. However, fast TRs (optical filters) are currently less mature. There are several ways to combat

the tuning overhead of currently available TRs. The aforementioned packet aggregation at each ring-and-star homed node allows for so-called *wormhole scheduling*, which compensates the relatively slow tuning speed of today's TRs [33]. Alternatively, two alternately operating TRs can be deployed such that one TR is used while the other one is tuning. In doing so, the tuning overhead is effectively masked. And finally, instead of a single fast TR, each ring-and-star homed node attached to the AWG-based star subnetwork can be equipped with an array of fixed-tuned transceivers, each operating at a separate wavelength channel, giving rise to various AWG-based star subnetwork architectures [34].

RINGOSTAR uses RPR's built-in source stripping for broadcasting and destination stripping in conjunction with shortest path routing to enable efficient bandwidth utilization by means of spatial reuse. The bidirectional ring provides fault tolerance against any single node or fiber failure on the ring. In addition, RINGOSTAR provides greater resilience to multiple path failures in the star subnetwork than stand-alone star networks. While in star networks, a fiber cut disconnects one or more nodes from the central hub; in RINGOSTAR, the ring can be used to protection-switch the traffic to other ring nodes whose intact star fibers can be shared by affected nodes. Compared with meshed rings, RINGOSTAR requires only a *single* wavelength router, which is sufficient to provide *single-hop* interconnection among all $N_{\rm rs}$ nodes. Note that in RINGOSTAR, the central AWG is quite reliable due to its passive nature, but forms a single point of failure of the star subnetwork. For survivability reasons, the AWG can be protected by a parallel load-sharing PSC [31]. Apart from possibly required optical amplifiers, the star subnetwork of RINGOSTAR containing only passive components (AWG, combiners, and splitters) is cost-effective, and the wavelength-insensitive splitters also enable optical multicasting.

We have seen in Section III that previously reported multichannel extensions of optical single-channel ring networks deployed WDM on the ring, resulting in meshed or nonmeshed WDM ring networks. Both meshed and nonmeshed WDM rings have in common that *all* ring nodes have to be WDM upgraded, be it by arrays of fixed-tuned transceivers, tunable transceivers, or wavelength multiplexers or demultiplexers. Nonmeshed WDM rings yield at most the same spatial reuse factor as their single-channel counterparts. To see this, note that for opaque WDM rings with O/E/O conversion at each node, the spatial reuse factor is the same in both nonmeshed WDM and single-channel rings. In WDM rings with optical bypassing, however, the spatial reuse factor in WDM rings can be smaller than in their single-channel counterparts. This is because optical bypassing makes the wavelength access less flexible and efficient since nodes can be addressed only on certain wavelengths, which do not necessarily provide the shortest path. As explained in Section III, for uniform traffic in bidirectional rings, the mean hop distance equals $N/4$, and the spatial reuse factor is upper bounded by four due to missing alternate physical short cuts. In RINGOSTAR, the spatial reuse factor of all WDM wavelength channels is given by the physical degree of the AWG D, which in principle can be chosen arbitrarily large (in practice, for large D, a free-space rather than planar AWG has to be used to provide a sufficiently small channel crosstalk). As a consequence, RINGOSTAR potentially achieves a much better WDM upgrade than conventional approaches that deploy WDM on the ring. Note that the parameter D together with S not only determine the number of ring-and-star homed nodes $N_{\rm rs} = D \cdot S$, but also the degree of spatial wavelength reuse on the ring. By using the concept of proxy stripping, data transmissions are bounded to smaller ring sections, resulting in a decreased mean hop distance, an increased number of simultaneous transmissions on different ring segments, and thus an increased spatial reuse factor on the ring. With properly chosen $D \cdot S$, the mean hop distance is smaller than $N/4$, and the spatial reuse factor on the ring can be pushed well beyond that of bidirectional rings (4) for uniform traffic. Clearly, there is a tradeoff between ring bandwidth reuse and network costs. With an increasing $N_{\rm rs}$, the spatial reuse factor on the ring improves and the costs of the network increase since more nodes require an additional tunable transceiver attached to the star via a separate fiber pair, and vice versa. Next, let us take a closer look at the impact of the parameters D and S on the performance of RINGOSTAR.

VI. Analysis and Results

In the following, we investigate the performance of RINGOSTAR in terms of mean hop distance, spatial reuse, and capacity by means of analysis. We also compare the performance of RINGOSTAR to that of unidirectional, bidirectional, and meshed ring networks, which deploy WDM on the ring as opposed to RINGOSTAR. Due to space constraints, we focus on uniform traffic, as typically found in metro core networks. For an analytical and simulative investigation of the throughput-delay performance of the network under uniform, hot-spot, symmetric, and asymmetric traffic demands, we refer the interested reader to our companion paper [35].

A. Mean Hop Distance

In the computation of the mean hop distance of RINGOSTAR, we assume uniform traffic, i.e., each node generates the same amount of traffic and a given data packet is destined to any of the $(N-1)$ nodes with equal probability $1/(N-1)$. (The assumption of uniform traffic is realistic in metro core networks with any-to-any traffic demands between central offices [30]. By assuming uniform traffic, we are also able to compare the mean hop distance of RINGOSTAR to that of unidirectional and bidirectional rings of (1) and (3), respectively.)

The mean hop distance $\overline{h}$ of RINGOSTAR is given by

$$\overline{h} = E[\text{hops}] \tag{5}$$

$$= \frac{1}{N(N-1)} \sum_{i=0}^{N-1} \sum_{j=0, j\neq i}^{N-1} \min\left\{ h^{\rm ring}_{\min_{i\_j}}, h^{\rm star}_{\min_{i\_j}} \right\} \tag{6}$$

$$= \frac{1}{N(N-1)} \sum_{i=0}^{N-1} \sum_{j=0, j\neq i}^{N-1} \min\left\{ h_{\min^{\rm ring}_{i\_j}}, h_{i\_{\rm rs}} + 1 + h_{j\_{\rm rs}} \right\}. \tag{7}$$

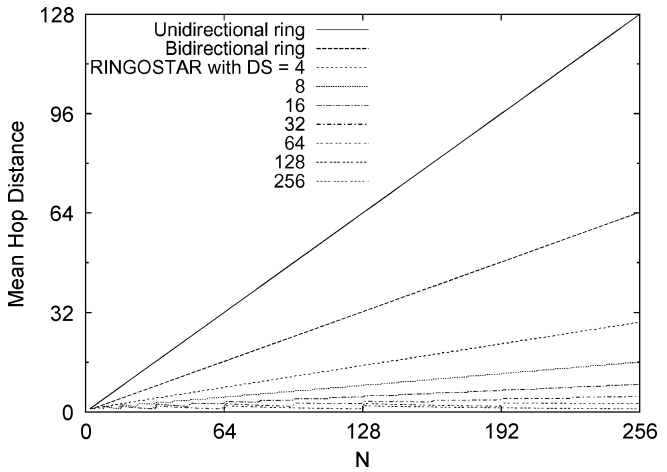

Fig. 6. Mean hop distance $\overline{h}$ of unidirectional ring with destination stripping, bidirectional ring with destination stripping and shortest path routing, and RINGOSTAR with different $D \cdot S \in \{4, 8, 16, 32, 64, 128, 256\}$ versus number of nodes N.

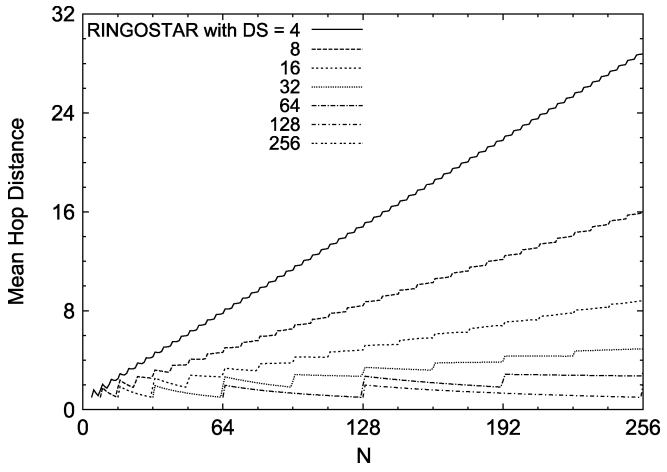

Fig. 7. Mean hop distance $\overline{h}$ of RINGOSTAR with different $D \cdot S \in \{4, 8, 16, 32, 64, 128, 256\}$ versus number of nodes N.

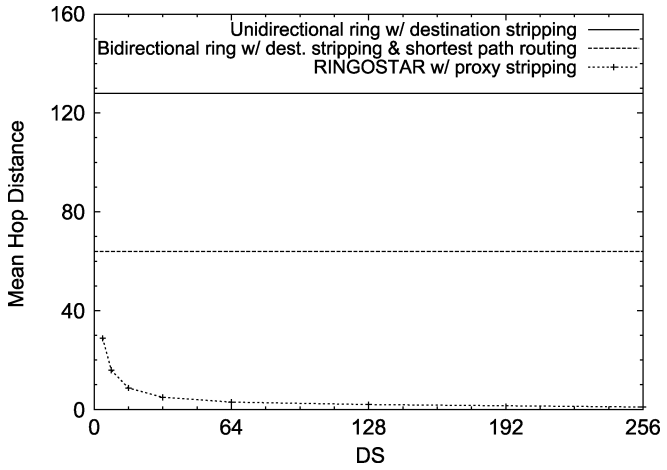

Fig. 8. Mean hop distance $\overline{h}$ of unidirectional ring with destination stripping, bidirectional ring with destination stripping and shortest path routing, and RINGOSTAR with proxy stripping versus $D \cdot S$ for $N = 256$.

By exploiting the architectural symmetry of RINGOSTAR, (7) becomes

$$\overline{h} = \frac{D \cdot S}{N(N-1)} \sum_{i=0}^{\frac{N}{D \cdot S}-1} \sum_{j=0, j \neq i}^{N-1} \min \left\{ h^{\text{ring}}_{\min_{i\_j}}, h_{i\_\text{rs}} + 1 + h_{j\_\text{rs}} \right\} \tag{8}$$

where

$$h^{\text{ring}}_{\min_{i\_j}} = \min \{ |i-j|, N - |i-j| \} \tag{9}$$

and

$$h_{l\_rs} = \min \left\{ l \bmod \frac{N}{D \cdot S}, \frac{N}{D \cdot S} - \left(l \bmod \frac{N}{D \cdot S} \right) \right\} \tag{10}$$

with $l \in \{i, j\}$.

Fig. 6 depicts the mean hop distance $\overline{h}$ versus the number of nodes N for RINGOSTAR with $D \cdot S \in \{4, 8, 16, 32, 64, 128, 256\}$, the unidirectional ring with destination stripping (see (1)), and the bidirectional ring with destination stripping and shortest path routing (see (3)). Clearly, for all types of network $\overline{h}$ increases with increasing N. However, note that the slope of the curves differs for the two rings and the various configurations of RINGOSTAR. The unidirectional ring features the largest mean hop distance and slope. Due to its dual-fiber structure and shortest path routing, the bidirectional ring provides a mean hop distance and slope that are approximately 50% smaller than those of the unidirectional ring. We observe from Fig. 6 that in RINGOSTAR $D \cdot S = 4$ ring-and-star homed nodes are sufficient to decrease the mean hop distance and slope significantly compared with unidirectional and bidirectional rings. A small mean hop distance improves the network capacity by alleviating the forwarding burden of each node. With a smaller slope, new nodes can be added to the network without deteriorating the mean hop distance significantly. As shown in Fig. 6, increasing the number of ring-and-star homed nodes $D \cdot S$ up to 64 further decreases $\overline{h}$. However, attaching more than 64 ring nodes to the central star does not further decrease $\overline{h}$ significantly. We observe that the curves of both unidirectional and bidirectional rings are linear while the mean hop distance $\overline{h}$ of RINGOSTAR is kind of step function of N. For convenience, the mean hop distance $\overline{h}$ of RINGOSTAR is depicted in greater detail in Fig. 7 with different $D \cdot S \in \{4, 8, 16, 32, 64, 128, 256\}$ versus number of nodes N (note that in the figure we have $\overline{h} = 1$ for $N = 256$). We observe that on each curve, $\overline{h}$ is increased if the number of nodes is equal to $N = n \cdot (D \cdot S) + 1$, where $n = 1, 2, \ldots, (N-1)/(D \cdot S)$. This is because whenever N exceeds an integer multiple of $D \cdot S$, the maximum hop distance (diameter) is increased by one, while further increasing N up to the next integer multiple of $D \cdot S$ does not increase the maximum hop distance. As a consequence, the mean hop distance $\overline{h}$ is increased whenever $N = n \cdot (D \cdot S) + 1$, where $n = 1, 2, \ldots, (N-1)/(D \cdot S)$. In the subsequent figures, we do not elaborate on these subtle details but highlight the main performance characteristics of RINGOSTAR by assuming that the number of nodes N is an integer multiple of $D \cdot S$, i.e., the number of ring homed nodes is the same between each pair of ring-and-star homed nodes.

Fig. 8, which depicts the mean hop distance $\overline{h}$ of RINGOSTAR versus the number of ring-and-star homed nodes $D \cdot S$ for a fixed number of nodes N (for comparison

TABLE I
MEAN HOP DISTANCE: NUMERICAL VALUES FOR $N = 256$

Network type	Mean hop distance
Unidirectional ring	128.0
Bidirectional ring	64.25
RINGOSTAR w/	
$D \cdot S = 4$	28.7941
$D \cdot S = 8$	15.9
$D \cdot S = 16$	8.7
$D \cdot S = 32$	4.91176
$D \cdot S = 64$	2.97059
$D \cdot S = 128$	1.98824
$D \cdot S = 256$	1.0

we also show $\overline{h}$ of both unidirectional and bidirectional rings, which are independent from $D \cdot S$, of course), confirms the previously mentioned fact that attaching more than 64 ring nodes to the central star does not further decrease the mean hop distance $\overline{h}$ of RINGOSTAR significantly. To demonstrate the potential of the proxy stripping technique, we choose a rather large value of $N = 256$, which is the maximum number of nodes supported by RPR. As mentioned previously, connecting only a few nodes to the central AWG-based star network helps RINGOSTAR outperform its ring counterparts clearly.

To quantify the benefit of proxy stripping, Table I lists the mean hop distance of both ring networks and RINGOSTAR with different $D \cdot S$ values for fixed $N = 256$. Due to destination stripping, the mean hop distance of the unidirectional ring is equal to 128, i.e., half the maximum hop distance. By using an additional counterdirectional fiber ring in conjunction with shortest path routing, the mean hop distance $\overline{h}$ is further reduced by a factor of approximately 2 in the bidirectional ring network, resulting in $\overline{h} = 64.25$. RINGOSTAR with $D \cdot S = 4$ achieves a mean hop distance of $\overline{h} = 28.7941$, which translates into a reduction of the mean hop distance by a factor of more than 2 compared with the bidirectional ring. Similarly, for $D \cdot S = 64$, the mean hop distance is equal to $\overline{h} = 2.97059$, which corresponds to an improvement by a factor of more than 21. Thus, by WDM upgrading only $(64/256) = 25\%$ of the ring nodes and attaching them to the star subnetwork, the mean hop distance is less than 5% of that of the bidirectional ring. Note that in RINGOSTAR, the minimum achievable mean hop distance $\overline{h} = 1.0$ is obtained if all 256 nodes are attached to the star subnetwork. In this case, each pair of source and destination nodes can communicate in one single hop at the expense of WDM upgrading and interconnecting all nodes via the star subnetwork.

B. Spatial Reuse and Capacity

The calculation of the capacity of RINGOSTAR is somewhat difficult since traffic generated in one subnetwork (either ring or star subnetwork) generally crosses over to the other subnetwork. As a consequence, the capacity of each subnetwork depends on the traffic coming from the other subnetwork. The capacity calculation of RINGOSTAR has to take this interdependence of both subnetworks into account properly. The capacity of RINGOSTAR is composed of the capacity of the ring subnetwork, C_r, and the capacity of the star subnetwork,C_s. According to [25], the capacity of each subnetwork C_{sub} is given by

$$C_{\text{sub}} = \frac{N_{\text{sub}} \cdot r_{\text{sub}} \cdot S_{\text{sub}}}{\overline{h}_{\text{sub}}} \tag{11}$$

where N_{sub} denotes the number of nodes of the subnetwork, r_{sub} denotes the number of transceivers at each subnetwork's node, S_{sub} denotes the line rate of each subnetwork's transceiver, and $\overline{h}_{\text{sub}}$ denotes the mean hop distance of the subnetwork. The interdependence of both subnetworks is accounted for by the $\overline{h}_{\text{sub}}$ of each subnetwork, as we will see shortly. By applying (11) to both ring and star subnetworks, the capacity of RINGOSTAR is obtained as follows:

$$C = C_r + C_s \tag{12}$$

$$= \frac{N \cdot r_r \cdot S_r}{\overline{h}_r} + \frac{D \cdot \min\{S \cdot r_s, R \cdot D\} \cdot S_s}{\overline{h}_s} \tag{13}$$

$$= \frac{2N \cdot S_r}{\overline{h}_r} + \frac{D \cdot \min\{S, R \cdot D\} \cdot S_s}{\overline{h}_s}. \tag{14}$$

To see this, note that in the star subnetwork S nodes, each equipped with $r_s = 1$ transceiver, are attached to each port of the $D \times D$ AWG. At each AWG port $R \cdot D$, wavelength channels are available for transmission/reception (recall from Section IV that R denotes the number of used FSRs of the underlying AWG). Thus, at each port of the $D \times D$ AWG up to $\min\{S, R \cdot D\}$, transmissions can take place simultaneously. To obtain the capacity of RINGOSTAR, we need to consider the interdependence of both subnetworks. To this end, we compute $\overline{h}_r$ and $\overline{h}_s$ next.

The mean hop distance of the ring subnetwork $\overline{h}_r$ is given by

$$\overline{h}_r = \frac{D \cdot S}{g_r} \sum_{i=0}^{\frac{N}{D \cdot S}-1} \sum_{j=0, j \neq i}^{N-1} h_r(i,j) \tag{15}$$

with

$$h_r(i,j) = \begin{cases} h^{\text{ring}}_{\min_{i\_j}} & \text{if } h^{\text{ring}}_{\min_{i\_j}} \leq h_{i\_\text{rs}} + 1 + h_{j\_\text{rs}} \\ h_{i\_\text{rs}} + h_{j\_\text{rs}} & \text{else} \end{cases} \tag{16}$$

and

$$g_r = D \cdot S \sum_{i=0}^{\frac{N}{D \cdot S}-1} \sum_{j=0, j \neq i}^{N-1} \text{Ind}\left\{\left(h^{\text{ring}}_{\min_{i\_j}} \leq h_{i\_\text{rs}} + 1 + h_{j\_\text{rs}}\right) \vee \left(h_{i\_\text{rs}} + h_{j\_\text{rs}} > 0\right)\right\} \tag{17}$$

where $\text{Ind}\{\cdot\}$ denotes the indicator function, and $h^{\text{ring}}_{\min_{i\_j}}$ and h_{l_rs}, $l \in \{i, j\}$, are given in (9) and (10), respectively.

The star subnetwork is a single-hop network with no intermediate forwarding nodes between any pair of source and destination ring-and-star homed nodes. Note, however, that the net line rate S_s of each ring-and-star homed node is decreased since each ring-and-star homed node is involved in proxy stripping data packets sent by its $((N/D \cdot S) - 1)$ adjacent ring homed nodes. Thus, each ring-and-star homed node has to forward proxy-stripped packets onto the star subnetwork. As a result, each ring-and-star homed node is able to send locally generated traffic only at an effective line rate of $S_s/\overline{h}_s$, where $\overline{h}_s$ denotes the mean number of nodes (both ring and

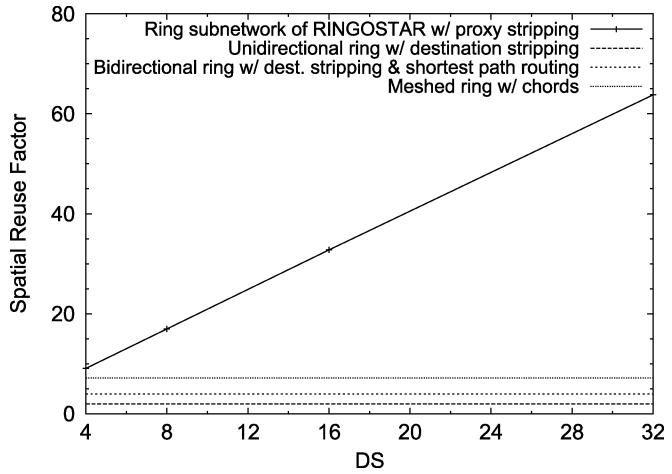

Fig. 9. Spatial reuse factor of ring subnetwork of RINGOSTAR with proxy stripping, unidirectional ring with destination stripping, bidirectional ring with destination stripping and shortest path routing, and meshed ring with chords versus $D \cdot S \in \{4, 8, 16, 32\}$ for $N = 256$.

ring-and-star homed nodes) that share the net line rate S_s of a given ring-and-star homed node. Accordingly, $\overline{h}_s$ is given by

$$\overline{h}_s = 1 + \frac{1}{N-1} \sum_{i=1}^{\frac{N}{D \cdot S}-1} \sum_{j=0, j \neq i}^{N-1} \mathrm{Ind}\left\{ h^{\mathrm{ring}}_{\mathrm{min}_{i\_j}} > h^{\mathrm{star}}_{\mathrm{min}_{i\_j}} \right\} \quad (18)$$

$$= 1 + \frac{1}{N-1} \sum_{i=1}^{\frac{N}{D \cdot S}-1} \sum_{j=0, j \neq i}^{N-1} \mathrm{Ind}\left\{ h^{\mathrm{ring}}_{\mathrm{min}_{i\_j}} > h_{i\_\mathrm{rs}} + 1 + h_{j\_\mathrm{rs}} \right\} \quad (19)$$

where $h^{\mathrm{ring}}_{\mathrm{min}_{i\_j}}$ and h_{l_rs}, $l \in \{i, j\}$ are given in (9) and (10), respectively.

The capacity of both ring and star subnetworks, C_r, C_s, and the total capacity of RINGOSTAR C are obtained by inserting (15) and (19) into (14). Note that the capacity of both subnetworks largely depends on the degree of spatial wavelength reuse. Clearly, in the star subnetwork, the spatial reuse factor is equal to the degree D of the underlying AWG. In the ring subnetwork, the spatial reuse factor is given by the ratio of number of internodal links and mean hop distance $N/\overline{h}_r$. Fig. 9 depicts the spatial reuse factor of the ring subnetwork of RINGOSTAR versus $D \cdot S \in \{4, 8, 16, 32\}$ for $N = 256$ and compares it with that of unidirectional, bidirectional, and meshed rings. We observe that the spatial reuse factor of the ring subnetwork increases with increasing $D \cdot S$. This is due to the fact that with more ring-and-star homed nodes, packet transmissions are restricted to smaller ring segments and thus consume fewer bandwidth resources. As a result, the mean hop distance decreases, and the spatial reuse factor increases on the ring subnetwork. Table II shows that in terms of spatial reuse of bandwidth, a rather small number of proxy stripping nodes $D \cdot S$ is sufficient for proxy stripping rings to clearly outperform unidirectional, bidirectional, and meshed rings. For instance, by adding proxy stripping capability to $(64/256) = 25\%$ of the ring nodes, RINGOSTAR's ring subnetwork achieves a spatial reuse factor of more than 120, which is dramatically larger than that of destination stripping unidirectional (2) and bidirectional (4) ring networks and meshed rings (7.2), as listed in Table II. The spatial reuse factor on the ring subnetwork of RINGOSTAR can

TABLE II
SPATIAL REUSE FACTOR: NUMERICAL VALUES FOR $N = 256$

Network type	Spatial reuse factor
Unidirectional ring	2
Bidirectional ring	4
Meshed ring	7.2
Ring subnetwork of RINGOSTAR w/	
$D \cdot S = 4$	9.10547
$D \cdot S = 8$	16.9854
$D \cdot S = 16$	32.7823
$D \cdot S = 32$	63.7778
$D \cdot S = 64$	120.567
$D \cdot S = 128$	192.251
$D \cdot S = 256$	256

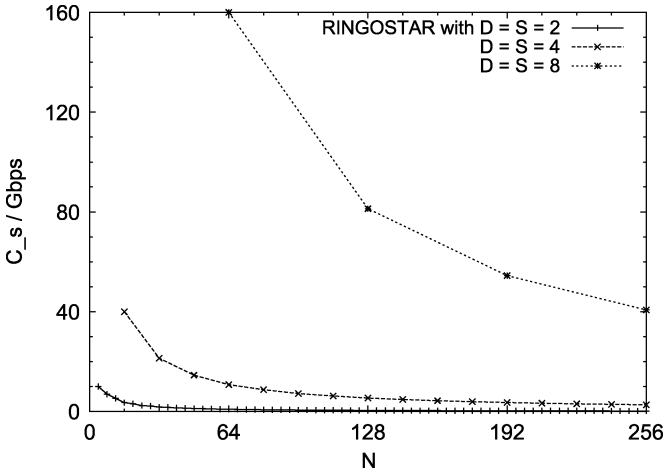

Fig. 10. Capacity C_s of star subnetwork of RINGOSTAR with $D = S$ and $D, S \in \{2, 4, 8\}$ versus number of nodes N for $S_s = 2.5$ Gb/s and $R \cdot D = 16$ wavelength channels.

be further increased by WDM upgrading additional ring nodes and attaching them to the central AWG-based star network (see Table II). Note that the maximum spatial reuse factor of $N = 256$ is obtained if all $N = 256$ nodes are attached to the star subnetwork. In this case, each node sends packets only to its two neighboring nodes via the ring subnetwork, while the remaining $N - 3 = 253$ nodes are reached across the star subnetwork, resulting in the minimum mean hop distance $\overline{h}_r = 1$. Thus, in general, proxy stripping rings are able to provide the maximum achievable spatial reuse factor of N at the expense of WDM upgrading and interconnecting all N nodes via the star subnetwork.

With proxy stripping, traffic is routed across the short cuts of the star subnetwork. As a consequence, the bandwidth of the star subnetwork is partly used for forwarding proxy-stripped data packets. Due to the forwarding, the capacity of the star subnetwork is decreased. Fig. 10 shows the impact of proxy stripping on the capacity C_s of the star subnetwork of RINGOSTAR with $D = S$ and $D, S \in \{2, 4, 8\}$ versus number of nodes N for $S_s = 2.5$ Gb/s and $R \cdot D = 16$ wavelength channels. (Assuming a typical channel spacing of 100 GHz, this requires that the transceivers attached to the star subnetwork are tunable over a range of 12 nm. For such a small tuning range, fast tunable electrooptic transceivers are promising candidates whose negligible tuning time of a few nanoseconds allow for tuning

on a per-packet basis.) We observe that with increasing D and S, C_s increases since more ring-and-star homed nodes are attached to the star subnetwork, with each proxy stripping traffic of a smaller number of ring homed nodes. All curves have in common that, with increasing N, the capacity C_s of the star subnetwork decreases. This is due to the fact that with a larger N, each ring-and-star homed node has to proxy strip traffic of a larger number of adjacent ring homed nodes $((N/D \cdot S) - 1)$. As a result, the capacity available for locally generated traffic is decreased. The capacity of the star subnetwork C_s could be increased by deploying more than $r_s = 1$ transceiver at each ring-and-star homed node and/or increasing the line rate S_s in order to provide additional bandwidth for sending traffic locally generated by ring-and-star homed nodes. Note that in metro edge networks, it might be sufficient to increase the number of transceivers r_s and/or line rate S_s of a *single* ring-and-star homed node, which acts as a hub node interconnecting the metro edge network to the metro core network. Since most edge traffic is outbound from the immediate localized region, metro edge networks exhibit strongly hubbed traffic patterns (hot spot) [30]. Upgrading only the hub ring-and-star homed node (hot spot) while operating the remaining $(D \cdot S - 1)$ ring-and-star homed nodes with a single transceiver offers a cost-effective way to provide efficient transport of the hubbed traffic demands via the short cuts of the star subnetwork of RINGOSTAR.

Figs. 9 and 10 show that increasing the number of ring-and-star homed nodes $N_{\rm rs} = D \cdot S$ significantly improves the spatial reuse factor of the ring subnetwork and the capacity of the star subnetwork, respectively, and thus the aggregate capacity of RINGOSTAR. However, not only do the number of ring-and-star homed nodes have an impact on the capacity of RINGOSTAR but also the way a given number of $N_{\rm rs}$ ring-and-star homed nodes are interconnected has an impact as well. Fig. 11 depicts the (aggregate) capacity C of RINGOSTAR versus number of nodes N with a fixed number of ring-and-star homed nodes $N_{\rm rs} = D \cdot S = 64$, line rates $S_s = S_r = 2.5$ Gb/s, and $R \cdot D = 16$ wavelength channels for different $D \in \{1, 2, 4, 8\}$. The $N_{\rm rs} = 64$ ring-and-star homed nodes are interconnected by a 2×2 AWG, 4×4 AWG, or 8×8 AWG. For comparison, we also consider the case $D = 1$. Note that for $D = 1$, the AWG is identical to a wavelength-insensitive PSC. The PSC is a broadcast device and does not allow for spatial wavelength reuse, as opposed to the wavelength-routing AWG. We observe from Fig. 11 that due to spatial wavelength reuse, the capacity of RINGOSTAR is larger if the ring-and-star homed nodes are interconnected by an AWG rather than a PSC. Moreover, with a larger D, the wavelength channels can be spatially reused at more ports, resulting in an increased capacity. Note that for $D = 4$ and $D = 8$, we obtain the same capacity. This is because for $D = 8$, only $S = 8$ ring-and-star homed nodes are attached to each AWG port. As a consequence, only 8 of 16 wavelength channels are used at each AWG port, preventing a further increase of the capacity. Note that the capacity of RINGOSTAR could be further increased by attaching more nodes to the star subnetwork and/or increasing the number of transceivers r_s and/or line rate S_s at each of the $N_{\rm rs}$ ring-and-star homed nodes, at the expense of higher equipment costs.

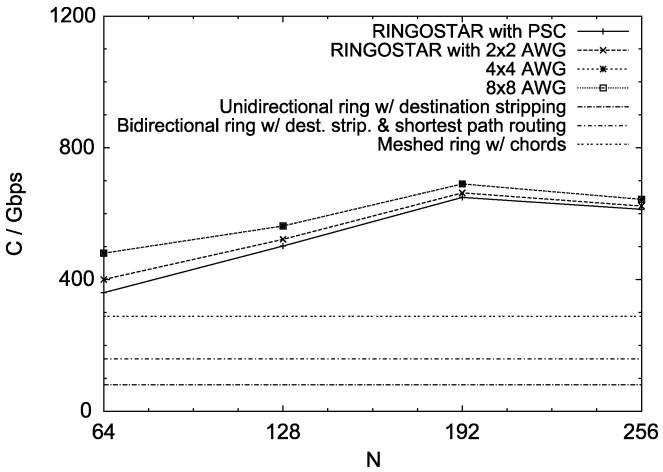

Fig. 11. Capacity C of RINGOSTAR versus number of nodes N with a fixed number of ring-and-star homed nodes $N_{\rm rs} = D \cdot S = 64$, line rates $S_s = S_r = 2.5$ Gb/s, and $R \cdot D = 16$ wavelength channels for different $D \in \{1, 2, 4, 8\}$.

To demonstrate the improved capacity of RINGOSTAR, we compare it with that of unidirectional ring with destination stripping, bidirectional ring with destination stripping and shortest path routing, and meshed rings with chords. Similar to RINGOSTAR, all three ring networks are assumed to use 16 wavelength channels. As opposed to RINGOSTAR, however, all N nodes of the ring networks are assumed to be WDM upgraded and be equipped with an array of 16 simultaneously operating transceivers, each fixed tuned to a separate wavelength. Fig. 11 illustrates that, in terms of capacity, RINGOSTAR with a *single* additional (tunable) transceiver at only $N_{\rm rs} = 64$ nodes dramatically outperforms unidirectional, bidirectional, and meshed WDM rings in which all $N = 256$ nodes need to be WDM upgraded by using an array of 16 (fixed-tuned) transceivers.

Finally, we note that the mean hop distance of RINGOSTAR depends only on the number of ring-and-star homed nodes $D \cdot S$. For a given $D \cdot S$, the mean hop distance of RINGOSTAR is the same for different combinations of D and S. The same holds for the spatial reuse factor of the ring subnetwork of RINGOSTAR. As indicated in Fig. 11, however, the capacity of RINGOSTAR depends heavily on the combination of D and S. More precisely, the capacity of the star subnetwork not only depends on D and S but also on D and the number of used FSRs R of the underlying AWG (see also (14)). Recall that $D \cdot R$ denotes the transceiver tuning range and thus the number of wavelength channels available at each AWG port. We next examine the impact of the number of used FSRs R and tuning range on the capacity of RINGOSTAR. Fig. 12 shows the capacity of RINGOSTAR versus number of nodes N with a fixed number of ring-and-star homed nodes $N_{\rm rs} = D \cdot S = 64$ and line rates $S_s = S_r = 2.5$ Gb/s for different AWG degrees $D \in \{2, 4, 8\}$ and number of used FSRs $R \in \{1, 2, 4\}$. Using a 2×2 AWG $S = 32$, ring-and-star homed nodes are attached to each AWG port. We observe from Fig. 12 that deploying more FSRs results in an increased capacity. By deploying only one FSR of a 4×4 AWG, we obtain the same capacity as for $D = 2$ and $R = 4$. This is because, in both cases, there is a total of $D^2 \cdot R = 16$ wavelength channels available, although with different transceiver tuning requirements. Specifically, with a $2 \times$

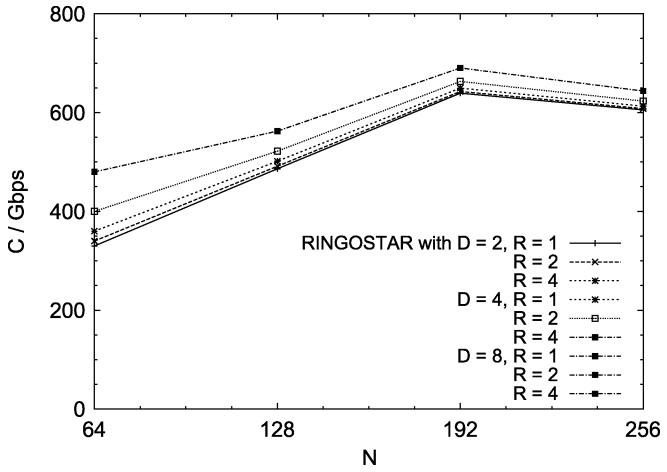

Fig. 12. Capacity C of RINGOSTAR versus number of nodes N with a fixed number of ring-and-star homed nodes $N_{\mathrm{rs}} = D \cdot S = 64$ and line rates $S_s = S_r = 2.5$ Gb/s for different $D \in \{2, 4, 8\}$ and $R \in \{1, 2, 4\}$.

2 AWG, each transceiver must be tunable over $D \cdot R = 8$ wavelength channels, while with a 4×4 AWG, each transceiver needs to be tunable only over $D \cdot R = 4$ wavelength channels, where each wavelength is spatially reused two and four times, respectively. Consequently, by means of spatial wavelength reuse, the number of required wavelength channels and thus the transceiver tuning range can be reduced in order to achieve the same network capacity. As shown in Fig. 12, the capacity of RINGOSTAR can be increased by exploiting more FSRs of the underlying 4×4 AWG, at the expense of a larger tuning range. Interestingly, using an 8×8 AWG instead of the 4×4 AWG does not result in any additional capacity increase, no matter how many FSRs are exploited. This is because with $D = 8$ (and $D \cdot S = 64$), only $S = 8$ ring-and-star homed nodes are attached to each AWG port for whom one FSR, i.e., eight wavelength channels, are sufficient to achieve the maximum capacity. Using mulitple FSRs is pointless since there are no ring-and-star homed nodes that could benefit from the additional wavelength channels. In summary, it appears to be the best choice to capitalize on spatial wavelength reuse by using a medium $D \in \{4, 8\}$ and to set the number of used FSRs R such that $D \cdot R = S$ in order to achieve a good tradeoff between capacity and required transceiver tuning range.

VII. Conclusion

This paper examined the multichannel extension of IEEE Standard 802.17 Resilient Packet Ring (RPR) in particular and optical single-channel ring networks in general by using wavelength-division multiplexing (WDM). Most previously reported multichannel extensions deploy WDM on the ring. All these WDM extensions have in common that all nodes have to be WDM upgraded, be it by arrays of fixed-tuned transceivers, tunable transceivers, wavelength multiplexers and demultiplexers. Furthermore, applying WDM on the ring achieves only a limited spatial reuse of wavelengths and thus a limited increase of capacity.

The proposed multichannel extension follows an entirely different direction to WDM upgrade RPR and optical single-channel ring networks. In the proposed approach presented in this paper, only a subset of ring nodes need to be upgraded with a single tunable transceiver. The subset of ring nodes are interconnected through a passive AWG-based wavelength-routing single-hop star network by using dark fibers that are abundantly available in metropolitan areas. Unlike previous multichannel extensions, WDM is deployed on the star subnetwork rather than on the ring. The resultant hybrid ring-star architecture, termed RINGOSTAR, provides an evolutionary and cost-effective dark-fiber WDM upgrade in that it builds on the single-channel network and node architecture. In doing so, RINGOSTAR benefits from the performance-enhancing techniques of RPR, e.g., destination stripping, shortest path routing, service differentiation, quality of service support, fairness control, electronic packet processing, and signal regeneration. Owing to its hybrid architecture, RINGOSTAR is able to combine the merits or ring topology (fault tolerance) and single-hop star topology (high bandwidth utilization and inherent transparency). By using the novel concept of proxy stripping, data packets are sent on single-hop short cuts across the star subnetwork. As a result, in RINGOSTAR, the overall mean hop distance is dramatically decreased, and the capacity is signficantly increased due to improved spatial wavelength reuse on both star and ring subnetworks. Specifically, by WDM upgrading and interconnecting only 64 nodes of a 256-node RINGOSTAR network, the mean hop distance is less than 5% of that of bidirectional rings with destination stripping and shortest path routing. In terms of capacity, a 256-node RINGOSTAR network with a single additional (tunable) transceiver at only 64 nodes significantly outperforms unidirectional, bidirectional, and meshed WDM rings in which each of the 256 nodes needs to be WDM upgraded by using an array of 16 (fixed-tuned) transceivers.

Clearly, the gained capacity comes at some expense. For increasing the capacity, a subset of nodes must be connected to the star subnetwork. Each of these nodes must be upgraded with tunable transceivers, and the access protocol of the star subnetwork requires additional processing capacity. Moreover, an AWG, splitters, and combiners must be deployed and interconnected by fibers. However, by means of analysis, it has been found that RINGOSTAR clearly outperforms unidirectional, bidirectional, and meshed ring networks—in which *all* nodes must be upgraded—in terms of mean hop distance, spatial reuse, and capacity. Therefore, RINGOSTAR is considered a more cost-effective solution, especially in the face of using dark fibers to build the star subnetwork. Another tradeoff between costs and performance concerns the additional delay introduced by the pretransmission coordination required for each transmission over the star subnetwork. The round-trip time of control packets on the peripheral ring could be avoided by deploying a passive star coupler in parallel with the AWG, at the expense of using an additional single passive component in the star subnetwork.

RINGOSTAR is well suited for efficiently transporting uniform traffic as present in metro core networks with any-to-any traffic demands between central offices. For metro edge networks with their strongly hubbed traffic patterns (hot spot), RINGOSTAR with its short cuts on the star WDM subnetwork

provides a promising cost-effective solution in that only the hub node (hot spot) is equipped with multiple transceivers while operating the remaining nodes with a single transceiver. Note that the RINGOSTAR WDM upgrade is not restricted to RPR. RINGOSTAR with its star WDM subnetwork and proxy stripping is generally applicable to asynchronous (e.g., token ring) and synchronous (e.g., empty slot) ring networks.

ACKNOWLEDGMENT

The authors would like to thank E. Modiano for fruitful discussions and insightful comments.

REFERENCES

[1] M. Maier, *Metropolitan Area WDM Networks—An AWG Based Approach*. Norwell, MA: Kluwer, 2003.
[2] R. Ramaswami and K. N. Sivarajan, *Optical Networks—A Practical Perspective*, 2nd ed. San Mateo, CA: Morgan Kaufmann, 2001.
[3] A. Hopper and R. C. Williamson, "Design and use of an integrated Cambridge ring," *IEEE J. Sel. Areas Commun.*, vol. SAC-1, no. 5, pp. 775–784, Nov. 1983.
[4] D. E. Huber, W. Steinlin, and P. J. Wild, "SILK: An implementation of a buffer insertion ring," *IEEE J. Sel. Areas Commun.*, vol. SAC-1, no. 5, pp. 766–774, Nov. 1983.
[5] I. Cidon and Y. Ofek, "MetaRing—a full-duplex ring with fairness and spatial reuse," *IEEE Trans. Commun.*, vol. 41, no. 1, pp. 110–120, Jan. 1993.
[6] P. Yuan, V. Gambiroza, and E. Knightly, "The IEEE 802.17 media access protocol for high-speed metropolitan-area resilient packet rings," *IEEE Network*, vol. 18, no. 3, pp. 8–15, May/Jun. 2004.
[7] *Resilient Packet Ring*, IEEE Standard 802.17, 2004.
[8] F. Kastenholz. (2002, Dec.) A Core Standard for Transmission of IP Packets Over IEEE 802.17 (Resilient Packet Ring) Networks. [Online]. Available: Internet Draft, draft-ietf-iporpr-core-00.txt
[9] M. Herzog, M. Maier, and M. Reisslein, "Metropolitan area packet-switched WDM networks: A survey on ring systems," *IEEE Commun. Surv.*, vol. 6, no. 2, pp. 2–20, 2nd Quarter 2004.
[10] K. V. Shrikhande, I. M. White, D.-R. Wonglumsom, S. M. Gemelos, M. S. Rogge, Y. Fukashiro, M. Avenarius, and L. G. Kazovsky, "HORNET: A packet-over-WDM multiple access metropolitan area ring network," *IEEE J. Sel. Areas Commun.*, vol. 18, no. 10, pp. 2004–2016, Oct. 2000.
[11] R. Gaudino, A. Carena, V. Ferrero, A. Pozzi, V. D. Feo, P. Gigante, F. Neri, and P. Poggiolini, "RINGO: A WDM ring optical packet network demonstrator," in *Proc., 27th Eur. Conf. Optical Communication (ECOC 2001)*, Amsterdam, The Netherlands, Oct. 2001, pp. 620–621.
[12] X. Zhang and C. Qiao, "An effective and comprehensive approach for traffic grooming and wavelength assignment in SONET/WDM rings," *IEEE/ACM Trans. Netw.*, vol. 8, no. 5, pp. 608–617, Oct. 2000.
[13] E. Modiano and R. Berry, "Using grooming cross-connects to reduce ADM costs in SONET/WDM ring networks," presented at the Optical Fiber Communication Conf. (OFC), vol. 3, 2001, Paper WL3, pp. WL3–1–WL3–3.
[14] E. Modiano and P. J. Lin, "Traffic grooming in WDM networks," *IEEE Commu. Mag.*, vol. 39, no. 7, pp. 124–129, Jul. 2001.
[15] D. Guo and A. S. Acampora, "Scalable multihop WDM passive ring with optimal wavelength assignment and adaptive wavelength routing," *J. Lightw. Technol.*, vol. 14, no. 6, pp. 1264–1277, Jun. 1996.
[16] W. Cho and B. Mukherjee, "Design of MAC protocols for DWADM-based metropolitan-area optical ring networks," in *Proc. IEEE GLOBECOM*, vol. 3, 2001, pp. 1575–1579.
[17] I. Rubin and H.-K. Hua, "An all-optical wavelength-division meshed-ring packet-switching network," in *Proc. IEEE INFOCOM*, vol. 3, Apr. 1995, pp. 969–976.
[18] ——, "SMARTNet: An all-optical wavelength-division meshed-ring packet-switching network," in *Proc. IEEE GLOBECOM*, vol. 3, Nov. 1995, pp. 1756–1760.
[19] M. Maier, M. Reisslein, and A. Wolisz, "A hybrid MAC protocol for a metro WDM network using multiple free spectral ranges of an arrayed-waveguide grating," *Comput. Netw.*, vol. 41, no. 4, pp. 407–433, 2003.
[20] M. Scheutzow, M. Maier, M. Reisslein, and A. Wolisz, "Wavelength reuse for efficient packet-switched transport in an AWG based metro WDM network," *J. Lightw. Technol.*, vol. 21, no. 6, pp. 1435–1455, Jun. 2003.
[21] M. S. Goodman, "Multiwavelength networks and new approaches to packet switching," *IEEE Commun. Mag.*, vol. 27, no. 10, pp. 27–35, Oct. 1989.
[22] ——, "Optical networks: new approaches to interconnection and switching," in *Conf. Dig., LEOS Summer Topical on Optical Multiple Access Networks*, Jul. 1990, pp. 13–14.
[23] A. M. Hill, M. Brierley, R. M. Percival, R. Wyatt, D. Pitcher, K. M. I. Pati, I. Hall, and J.-P. Laude, "Multiple-star wavelength-router network and its protection strategy," *IEEE J. Sel. Areas Commun.*, vol. 16, no. 7, pp. 1134–1145, Sep. 1998.
[24] W.-P. Lin, M.-S. Kao, and S. Chi, "The modified star-ring architecture for high-capacity subcarrier multiplexed passive optical networks," *J. Lightw. Technol.*, vol. 19, no. 1, pp. 32–39, Jan. 2001.
[25] A. S. Acampora and S. I. A. Shah, "Multihop lightwave networks: A comparison of store-and-forward and hot-potato routing," in *IEEE INFOCOM*, vol. 1, Apr. 1991, pp. 10–19.
[26] F. Davik, M. Yilmaz, S. Gjessing, and N. Uzun, "IEEE 802.17 resilient packet ring tutorial," *IEEE Commun. Mag.*, vol. 42, no. 3, pp. 112–118, Mar. 2004.
[27] C. Fan, M. Maier, and M. Reisslein, "The AWG||PSC network: A performance enhanced single-hop WDM network with heterogeneous protection," in *Proc. IEEE INFOCOM*, vol. 3, San Francisco, CA, Mar./Apr. 2003, pp. 2279–2289.
[28] CANARIE (2005). *http://www.canarie.ca/* [Online]
[29] N. Ghani, "Metropolitan networks: Trends, technologies, and evolutions," in *Proc., IEEE Int. Conf. Communications (ICC)*, New York, NY, Apr. 28–May 2, 2002.
[30] I. P. Kaminow and T. Li, Eds., *Optical Fiber Telecommunications*. New York: Academic , 2002, vol. IVB, ch. 8, pp. 329–403.
[31] C. Fan, M. Maier, and M. Reisslein, "The AWG||PSC network: A performance-enhanced single-hop WDM network with heterogeneous protection," *J. Lightw. Technol.*, vol. 22, no. 5, pp. 1242–1262, May 2004.
[32] K. Shrikhande, I. M. White, M. S. Rogge, F.-T. An, A. Srivatsa, E. S. Hu, S. S.-H. Yam, and L. G. Kazovsky, "Performance demonstration of a fast-tunable transmitter and burst-mode packet receiver for *HORNET*," presented at the Proc. Optical Fiber Communication Conf. (OFC), vol. 4, 2001, Paper ThG2, pp. ThG2–1–ThG2–3.
[33] D. Guo, Y. Yemini, and Z. Zhang, "Scalable high-speed protocols for WDM optical star networks," in *Proc. IEEE INFOCOM*, vol. 3, Jun. 1994, pp. 1544–1551.
[34] M. Maier and M. Reisslein, "AWG based metro WDM networking," *IEEE Commun. Mag.*, vol. 42, no. 11, pp. S19–S26, Nov. 2004.
[35] M. Herzog, S. Adams, and M. Maier, "Proxy stripping: A performance enhancing technique for optical metropolitan area ring networks," *OSA J. Optical Networking*, Mar. 2005, submitted for publication.

Martin Herzog received the Dipl.Ing. degree (with distinctions) in computer engineering from the Technical University Berlin, Berlin, Germany, in 2002. He is currently working toward the Ph.D. degree at the Telecommunication Networks Group of the Technical University Berlin, where he participates in a graduate, interdisciplinary engineering research program.

His research interests lie in the area of optical wavelength-division-multiplexing (WDM) networks with a focus on architectures and access protocols for metro networks.

Martin Maier (M'03) received the Dipl.Ing. and the Dr.Ing. degrees (both with distinctions) in electrical engineering from the Technical University Berlin, Berlin, Germany, in 1998 and 2003, respectively.

He was a Visiting Researcher at the University of Southern California (USC), Los Angeles, and Arizona State University (ASU), Tempe. In summer 2003, he was a Postdoc Fellow at the Massachusetts Institute of Technology (MIT), Cambridge. Currently, he is a Research Associate at Centre Tecnològic de Telecomunicacions de Catalunya (CTTC), Barcelona, Spain. He is the author of the book *Metropolitan Area WDM Networks—An AWG Based Approach* (Norwell, MA: Kluwer, 2003). His research interests include network and node architectures, routing and switching paradigms, protection, multicasting, and the design, performance evaluation, and optimization of MAC protocols for optical wavelength-division-multiplexing (WDM) networks, automatically switched optical networks (ASONs), and generalized multiprotocol label switching (GMPLS), with particular focus on metro and access networks. Recently, his research interests have concentrated on evolutionary WDM upgrades of optical metro ring networks and access networks.

Dr. Maier was a recipient of the two-year Deutsche Telekom doctoral scholarship from June 1999 through May 2001. He is also a co-recipient of the Best Paper Award presented at The International Society for Optical Engineers (SPIE) Photonics East 2000—Terabit Optical Networking Conference.

Adam Wolisz (M'94–SM'99) received the Dipl.Ing degree in control engineering and the Dr.Ing. and Habilitation degrees, both in computer engineering, from the Silesian Technical University, Gliwice, Poland, in 1972, 1976, and 1983, respectively.

He was previously with the Polish Academy of Science (1972–1989), where he led activities on networking, and GMD Fokus (1990–1993), where he led activities on quantitative aspects of high-speed networks and multimedia systems. From 2001 to 2003, he was the dean of the Faculty of Electrical Engineering and Computer Science of the Technical University Berlin (TUB), Berlin, Germany. He was also a Member of Directorial Board of the Fraunhofer Institute for Open Communication Systems (FhG Fokus). He is currently the chaired Professor of Electrical Engineering and Computer Science at TUB, where he is heading the Telecommunication Network Group and the Institute of Telecommunication Systems. He has authored two books and authored or coauthored over 100 papers in technical journals and conference proceedings. His research interests are in architectures and protocols of communication networks as well as protocol engineering with an impact on performance and quality of service aspects. Currently, he is working mainly on mobile multimedia communication, with special regard to architectural aspects of network heterogeneity and wireless/mobile Internet access.

Dr. Wolisz is a Member of Informationstechnische Gesellschaft (ITG).